PNAS
www.pnas.org

Supplementary Appendix for:

Clostridioides difficile infection damages colonic stem cells *via* TcdB, impairing epithelial repair and recovery from disease.

Steven J. Mileto[1 †], Thierry Jardé[2, 3 †], Kevin O. Childress[4 †], Jaime L. Jensen[4], Ashleigh P. Rogers [1], Genevieve Kerr[2], Melanie L. Hutton[1], Michael J. Sheedlo[4], Sarah C. Bloch[4], John A. Shupe[4], Katja Horvay[2], Tracey Flores[2], Rebekah Engel[2, 5], Simon Wilkins[5, 6], Paul J. McMurrick[5], D. Borden Lacy[4,5*†], Helen E. Abud[2, 5, 6*†] and Dena Lyras[1*†].

Affiliations:

[1] Infection and Immunity Program, Monash Biomedicine Discovery Institute and Department of Microbiology, Monash University, Clayton, Victoria, Australia, 3800.

[2] Development and Stem Cells Program, Monash Biomedicine Discovery Institute and Department of Anatomy and Developmental Biology, Monash University, Clayton, Victoria, Australia, 3800.

[3] Centre for Cancer Research, Hudson Institute of Medical Research, Clayton VIC, Australia.

[4] Department of Pathology, Microbiology and Immunology, Vanderbilt University Medical Center, Nashville, TN, USA 37232.

[5] The Veterans Affairs Tennessee Valley Healthcare System, Nashville, TN, USA 37232.

[6] Department of Epidemiology and Preventive Medicine, School of Public Health and Preventive Medicine, Monash University, VIC 3004, Australia

[†] These authors contributed equally.

* Correspondence to: Dena Lyras, Helen Abud and D. Borden Lacy

Email: dena.lyras@monash.edu, helen.abud@monash.edu and borden.lacy@vanderbilt.edu.

This PDF file includes:

www.pnas.org/cgi/doi/10.1073/pnas.1915255117

Supplementary Materials and Methods

Bacterial strains, and growth conditions

C. difficile strains (see Table S1) were cultured on HIS-T agar (heart infusion (HI) (Oxoid) supplemented with 1.5% glucose, 0.1% (w/v) L-cysteine, 1.5% (w/v) agar and 0.1% (w/v) sodium taurocholate (New Zealand Pharmaceuticals)), prior to inoculation into 500 mL Tryptone Yeast (TY) broth (3% tryptone (Oxoid), 2% yeast extract (Oxoid) and 0.1% sodium thioglycolate (Sigma-Aldrich)) and grown for seven days anaerobically at 37°C. Spores were harvested by centrifugation at 10,000 *g* for 20 minutes at 4°C, washed eight times with chilled dH_2O and resuspended in Phosphate Buffered Saline (PBS) containing 0.05% Tween-80 (PBS-T) prior to heat-shocking at 65°C for 20 minutes.

Cell Lines and Reagents

HEK293 STF cells were a gift from Dr. J. Nathans (Johns Hopkins University) and were maintained in Dulbecco's Modified Eagle's medium, high glucose (Gibco) with 8% FBS. All cells were grown in a humidified incubator at 37°C with 5% CO_2 atmosphere.

Recombinant protein cloning, expression and purification.

Site directed mutagenesis was used to generate VPI10463 $TcdB^{GFE}$ (pBL881) in pHis1622-VPI10463-TcdB-C-term-8X-His (pBL377) with primers F-GAAAGTATGAATATAAAAAGTATTTTCGGATTCGAGAATATTAAGTTTATA and R-CTTATTATAAAATTAGCATCTAATATAAACTTAATATTCTCGAATCCGAAAATACTTTTTAT. pHis1622-M7404-TcdB-C-term-6X-His plasmid (pBL598) was a gift from Dr. J. Ballard (University of Oklahoma Health Sciences Center). Recombinant TcdB proteins were expressed in *Bacillus megaterium* and purified as previously described (1).

PNGase F expression vector pOPH6 (pBL831) was a gift from Shaun Lott (Addgene plasmid # 40315). pOPH6 was transformed into *E. coli* BL21 DE3 cells. Overnight cultures were prepared in 5 mL Luria Broth (LB) at 37°C and inoculated into 250 mL LB the following day. This

culture was shaken at 220 rpm at 37°C and grown to an OD_{600} of 0.6. Expression of PNGase F was induced with 0.25 mM IPTG, followed by an overnight incubation at 18°C. PNGase F was purified as outlined (2).

FZD2-CRD (residues 24-156), CSPG4 (residues 400-764), and NECTIN-3 (residues 58-302) DNA was cloned into pCDNA3.4 with an N-terminal human serum albumin secretion peptide (MKWVTFISLLFLFSSAYS) and a C-terminal TEV protease site and 6X-His tag (Thermo Fisher Scientific) to generate the plasmids pBL808, pBL790, and pBL787 respectively. The receptors were expressed in ExpiCHO cells (Thermo Fisher Scientific) in 25 mL according to the manufacturer's protocol. ExpiCHO supernatant was collected, and receptors were purified using cobalt-nitriloacetic acid resin (GE) and concentrated to 1 mL using 3 kDa or 10 kDa molecular weight cutoff filters (MilliporeSigma). FZD2-CRD and CSPG4 were treated with a 1:10 molar ratio of PNGaseF to receptor for 16 hours at 37°C. The receptors were further purified using size exclusion chromatography with an S-75 column. The receptors were stored in 20 mM HEPES pH 8.0, 100 mM NaCl.

Microscale Thermophoresis

Microscale thermophoresis (MST) experiments were performed on a NanoTemper Monolith NT.115 (NanoTemper Technologies GmbH, Munich, Germany). VPI $TcdB_{10463}$, $TcdB_{027}$, VPI $TcdB_{10463}^{GFE}$, FZD2-CRD, CSPG4, and NECTIN-3 were equilibrated prior to labelling with size exclusion chromatography using either a Superdex 200 10/300 or Superdex 75 10/300 column (GE) with 20 mM HEPES pH 8.0, 100 mM NaCl. Toxins, CSPG4, and NECTIN-3 were labelled with the Monolith NT His-tag Labelling Kit RED-tris-NTA, following the manufacturer's instructions. TcdB or receptor concentration was held constant at 50 nM. Serial dilutions of FZD2-CRD or TcdB were prepared using a 1:1 dilution from 3-10 µM to 90-300 pM in 20 mM HEPES pH 8.0, 100 mM NaCl, 0.05% Tween-20, and protease inhibitor cocktail for His-tagged proteins (Sigma). Samples were loaded into Monolith NT.115 capillaries (NanoTemper), and measurements carried out at 21°C with 40% MST power and 60% excitation power. MO.Control v1.6 was used for data collection, and MO.Affinity Analysis v2.3 and PALMIST were used for data analysis (3). The K_D constants were

calculated in PALMIST utilizing the saturation binding curve at equilibrium.

Animal model of *C. difficile* infection

Animal handling and experimentation was performed according to Victorian State Government regulations, approved by the Monash University Animal Ethics Committee (Monash University AEC no. SOBSB/M/2010/25 and MARP/2014/135). Time-course animal infections were conducted using the Monash mouse model of CDI as previously described (4, 5), with the following modifications. Three days prior to infection, at the completion of the seven day antibiotic cocktail pre-treatment described previously (4, 5), mice were switched to water containing cefaclor (300 µg/mL), *ad libitum*, and returned to untreated water on the day of infection. Male, six to eight week old, C57BL/6J mice (Walter and Eliza Hall Institute of Medical Research) were challenged with 10^6 spores of a single strain of *C. difficile* by gastric inoculation and were monitored twice daily as described previously for disease signs (including weight loss, behavioral changes and diarrhea) (5). For the time course of infection experiments, mice were euthanized at either 12, 24 or 48-hours post-infection or upon reaching the following endpoints for the genetically diverse strains comparison: acute weight loss of greater than 10% relative to the day of infection (day zero) in the first 24-hours or chronic weight loss of greater than 15% relative to day zero thereafter, or on animals becoming moribund, showing low activity, labored breathing, severe diarrhea, and a scruffy coat. For the recovery model of infection, mice that reached a weight loss of greater than 10% relative to the day of infection but less than 15% relative to day zero at the peak of infection (48-hours) were allowed to recover for either 7 days or 14 days before being euthanized. Fecal pellets were collected from all animals and resuspended at 100 mg/mL in sterile PBS before culturing on supplemented Heart Infusion agar, as previously described (4). Weight loss relative to day zero (D0) was plotted for each group/time-point and analyzed with Graph Pad Prism 7 using a one-way ANOVA and Tukey's test. For the panel of clinical and animal *C. difficile* strains, feces collected at 24 hours post infection was further diluted to 50 mg/ml in PBS. The diluted feces were used to determine toxin levels within the infected mice. To do this, these preparations were filter sterilized using 0.45 µm and 0.22 µm filters (Sartorius) and two-fold serial dilutions of the fecal supernatants

were prepared in Minimal Essential Medium (MEM) α (Gibco, ThermoFisher Scientific) or McCoy's 5A (modified) Medium (Gibco, ThermoFisher Scientific) supplemented with 1% (v/v) heat inactivated fetal calf serum (HI-FCS). Vero and HT-29 cells were cultured and prepared as previously described (6). Cells were seeded in 96-well plates at 1×10^4 cells/well, and incubated for 24 hours at 37°C in 5% CO_2 prior to exposing these cells to the filtered fecal content. All conditions were prepared in technical duplicated and at least four biological replicates. Morphological changes were observed after 18 hours using an Olympus 1X71 inverted microscope at 20x magnification. The toxin titre was evaluated as the final dilution at with 100% cell rounding, in comparison to the negative control wells, and was scored before analyzing with Graph Pad Prism 7 using a Mann-Whitney *U* test.

Four micron sections of formalin fixed (10% neutral buffered), Swiss-rolled colon and caecum were periodic acid–Schiff/Alcian blue stained by the Monash Histology Platform and assessed using a previously described scoring system (5). Stained sections were scanned for visualization using an Aperio Scanscope AT Turbo, at 20x magnification. For recovery mice, crypt length was measured for 30 crypts/mouse at equal points across the entire length of the colon, using the measure tool within Aperio ImageScope. All histopathological analysis was performed blind and analyzed with Graph Pad Prism 7 using a Mann-Whitney *U* test.

Animal model of *C. difficile* intoxication

All mouse experiments were approved by Vanderbilt Institutional Animal Care and Use Committee (IACUC). Female, five to eight-week old C57BL/6 mice (Jackson Laboratories) were housed five to a cage with free access to food and water. After a four-day acclimation period, mice were switched to water containing cefoperazone (500 µg/mL) for five days, with changes every 48-hours. After five days, cefoperazone treated water was switched back to untreated water and a 48-hour recovery period was allowed before being intoxicated with a 200 µL volume of 50 µg TcdB (VPI10463, VPI10463 GFE, or 027) or PBS as a control.

For the intoxication procedure, mice were anesthetized with isoflurane. A 21 gauge flexible gavage was inserted approximately 2 cm in *via* the rectum and each condition was slowly

administered. Rectal pressure was applied for 30 seconds to prevent immediate leakage, and mice were placed in a clean cage to recover. After four hours, the mice were euthanized by CO_2 gas, the abdomens were opened up, and colons extracted. Each colon was flushed with PBS, Swiss-rolled, and fixed in 10% formalin. After embedding in paraffin, the colonic tissue was sliced, mounted to a microscope slide, and stained with H&E by the Translational Pathology Shared Resource (TPSR) center at Vanderbilt University Medical Center. The tissue was then scored for edema, inflammation, and epithelial injury as previously described (7) by a pathologist blinded to the experimental conditions.

Immunohistochemistry and Immunofluorescence analysis

Paraffin-embedded colonic tissues were processed using standard procedures. Slides were de-waxed and antigen retrieval was performed using 10 mM citrate (Sigma-Aldrich) buffer, with 0.05% Tween-20 (Amresco), pH 6.0. Slides were blocked for 60 minutes with CAS-Block™ (Thermo-Fisher Scientific) at room temperature. For immunofluorescence staining, slides were incubated with either mouse anti-ezrin (Thermo-Fisher Scientific; 1:200 dilution in 1% Bovine serum albumin (BSA; Sigma Aldrich) in PBS) or mouse anti-β-catenin (BD; 1:200 dilution in 1% BSA) and rabbit anti-E-cadherin (Cell Signaling; 1:200 dilution in 1% BSA) overnight at 4°C. Slides were rinsed three times in PBS before incubation with secondary antibodies for 60 minutes at room temperature. For ezrin and β-catenin, goat anti-mouse IgG, Alexa Fluor® 488 (Thermo-Fisher Scientific; 1:1000 dilution in 1% BSA) was used, for E-cadherin goat anti-rabbit IgG, Alexa Fluor® 568 (Thermo-Fisher Scientific; 1:1000 dilution in 1% BSA) was used. Slides were washed three times in PBS before staining the nuclei with DAPI (300 nM, Thermo Fisher). Slides were mounted with ProLong® Gold (Thermo Fisher), sealed and imaged using a Leica SP8 Confocal Invert microscope on a 20x/1.0 oil objective with LasX Software (Leica).

For immunohistochemical staining for activated caspase-3, dewaxing, antigen retrieval and blocking was performed as above. Slides were then incubated overnight with rabbit anti-cleaved caspase-3 antibody (Cell Signaling; 1:250 dilution). Slides were rinsed three times in PBS before secondary antibody incubation for 60 minutes at room temperature with HRP conjugated goat anti-

rabbit IgG (Thermo-Fisher Scientific; 1:200 dilution). All antibodies were diluted in 1% BSA in PBS. Slides were washed three times, before incubating with 3,3'-Diaminobenzidine (DAB) reagent (Dako) for up to five minutes, until color developed. Slides were immediately washed three times in PBS before staining the nuclei with Mayer's Haematoxylin (Amber Scientific) for three minutes prior to washing and mounting with D.P.X. Stained sections were scanned for visualization using an Aperio Scanscope AT Turbo, at 20x magnification. Caspase-3 positive cells were counted per 700 µm field of view. Counts of cells positive for activated caspase-3 were graphed with GraphPad Prism 7, and tested for statistical differences using a Mann-Whitney *U* test.

Colonic stem cell sorting and quantitative PCR for stem cell and TcdB receptors

Mouse colonic crypt isolation and organoid establishment were based on protocols previously described (8-10). Intact, dissected colons from adult LGR5-eGFP-IRES-CreERT2 mice (11) (a pool of 10 colons was used per biological replicate) were flushed with 50 mL of cold PBS to remove luminal contents, cut longitudinally and scraped with a glass cover slip to remove epithelial fragments, mucus and feces. Colons were cut into 5 mm pieces and washed in cold PBS before digestion with 4 mM EDTA. To isolate crypts, the tissue fragments were vigorously suspended in cold PBS using a 10 mL pipette. This procedure was repeated a total of three times. Crypts were pelleted by centrifugation at 240 *g* for five minutes, at 4°C. The collected crypts were then dissociated in TrypLE Express (Invitrogen) supplemented with 10 µM Y-27632 Rock inhibitor (Abcam) and DNAse 1 (Sigma-Aldrich) for four minutes at 37°C. Cell clumps and mucus were removed using a 70 µm cell strainer (BD Biosciences). The remaining dissociated cells were washed twice with PBS and collected by centrifugation at 4°C at 240 *g* for five minutes. Antibody labelling step as well as the final resuspension of the sample were performed with PBS supplemented with 2 mM EDTA, 2% FBS and 10 µM Y-27632 Rock inhibitor. As previously described (9), cellularized crypts were incubated with anti-CD31-BV510 (1:200, clone: MEC 13.3, BD Horizon), anti-CD45-BV510 (1:200, clone: 30-F11, BD Horizon) and anti-CD24-PeCy7 (1:100, clone: M1/69, eBioscience) antibodies in a 500 µL volume for 15 minutes on ice. After washing twice with PBS, the cells were resuspended in a final volume of 1 mL, passed through a 70 µm

strainer and transferred into appropriate FACS tubes containing propidium idodine (PI) at a concentration of 2 µg/mL. Cell sorting was carried out with a 100 µm nozzle on an Influx instrument (BD Biosciences). Aggregates, debris, dead cells (PI+), and CD45+/CD31+ hematopoietic/endothelial contaminates were depleted. For the LGR5-GFP^{high} cell population, around 2% of the CD24^{+} LGR5-GFP brightest cells were selected. The subsequent 2% of the CD24^{+} LGR5-GFP+ cells were considered as LGR5-GFP^{med} and LGR5-GFP^{low} cell populations. A fully differentiated cell population, identified as CD24- LGR5-, was also isolated. Purity of collected fractions was confirmed by reanalysis of a small fraction of the sorted cells.

Following FACS, cells were centrifuged at 240 *g* for five minutes at 4°C and resuspended in RLT buffer. RNA was then extracted using the Qiagen RNeasy Microkit following the manufacturer's instructions, and used to synthesize cDNA, using a QuantiTect Reverse Transcription kit (Qiagen), using 70 ng of RNA. The cDNA was quantified using the QIAExpert prior to dilution for use in quantitative PCR (qPCR). The qPCR was conducted as previously described (12), normalizing to β-2-microglobulin (*B2m*) and β-actin (*Actb*), using the corresponding forward and reverse primers: *Actb,* F-TGTTACCAACTGGGACGACA, R-GGGGTGTTGAAGGTCTCAAA; *B2m*, F-CTTTCTGGTGCTTGTCTCACTG, R-AGCATTTGGATTTCAATGTGAG; *Cspg4*, F-CCTGGTAGGCTGCATAGAAGAT, R-CCAGGGTGGAGAAAGTTTCATA; *Fzd7*, F-AGAGATTTGGGGCGAGAGAT, R-CAGTTAGCATCGTCCTGCAA; *Lgr5*, F-CCTTGGCCCTGAACAAAATA, R-ATTTCTTTCCCAGGGAGTGG; *Lrp1,* F-GACCAGGTGTTGGACACAGATG, R-AGTCGTTGTCTCCGTCACACTTC; *Nectin3,* F-TTGCCCTTTCCTTTGTCAAC, R-GCATGTCTGATGGTGGAATG.

RNA extraction, cDNA preparation and digital droplet PCR-analysis

Colonic tissues collected from infected mice were placed in RNA*later*™ (Ambion) prior to RNA extraction. The tissues were then homogenized and total RNA was extracted using the RNeasy mini kit (Qiagen). One microgram of RNA was used for cDNA synthesis using a QuantiTect Reverse Transcription kit (Qiagen). The cDNA was quantified using the QIAExpert prior to dilution for use in digital droplet PCR (ddPCR). The ddPCR was conducted as previously described (12),

normalizing to β-2-microglobulin (*B2m*), using the corresponding forward and reverse primers, as follows:

Ascl2, F-CAGGAGCTGCTTGACTTTTCCA, R-GGGCTAGAAGCAGGTAGGTCCA; *Axin1*, F-GCAGCTCAGCAAAAAGGGAAAT, R-TACATGGGGAGCACTGTCTCGT; *B2m*, F-CTTTCTGGTGCTTGTCTCACTG, R-AGCATTTGGATTTCAATGTGAG; *Bmi1*, F-ATGCATCGAACAACCAGAATC, R-GTCTGGTTTTGTGAACCTGGA; *c-myc*, F-CTAGTGCTGCATGAGGAGACAC, R-GTAGTTGTGCTGGTGAGTGGAG; *Ephb2*, F-AGAATGGTGCCATCTTCCAG, R-GCACATCCACTTCTTCAGCA; *Fzd7*, F-AGAGATTTGGGGCGAGAGAT, R-CAGTTAGCATCGTCCTGCAA; *Lgr5*, F-CCTTGGCCCTGAACAAAATA, R-ATTTCTTTCCCAGGGAGTGG.

Following this, ddPCR was performed using 2x QX200 ddPCR EvaGreen Supermix (Bio-Rad), and 100 nM of each corresponding forward and reverse primer, as above. For each PCR reaction variable quantities of template cDNA were used (target gene dependent), with each reaction being performed in a final volume of 25 µL. From this, 20 µL was added to a DG8™ Cartridge for droplet generation using QX200 Droplet Generation Oil for EvaGreen (Bio-Rad). The generated droplets were transferred to a 96-well PCR-plate (Eppendorf) and subjected to thermo-cycling as previously described (12). Transcript levels were quantified and adjusted to copies per 10 µg of cDNA before normalizing to the housekeeping gene *B2m*. The adjusted transcript levels were plotted as a fold-change relative to uninfected using GraphPad Prism 7, with statistical significance assessed using a Mann Whitney *U* test.

Growth of murine colonic-organoids from *C. difficile* infected mice

Mouse colonic crypt isolation and organoid establishment were based on protocols previously described (8, 9). Intact, dissected colons from C57BL/6J mice (MARP) were flushed and scraped, as above. Colons were cut into 5 mm pieces and washed in cold PBS before digestion with 4 mM EDTA. Crypts were isolated from the tissues through vigorous re-suspension in cold PBS using a 10 mL pipette. This procedure was repeated a total of three times. Crypts were pelleted by centrifugation at 240 *g* for five minutes, at 4°C. The crypt pellet was resuspended in PBS, passed

through a 70 µm cell strainer (BD) and centrifuged. The supernatant was discarded and the pellet containing the crypts was resuspended in matrigel (BD). Equal numbers of crypts in matrigel were seeded into each well of a 48-well plate (Nunc) and incubated for 10 minutes at 37°C until solidified. Crypt culture media (DMEM/F12 supplemented with B27 (Gibco), Glutamax (Gibco), N2 (Gibco), 10 mM HEPES (Gibco), Fungizone (Gibco), 50 ng/mL EGF (Peprotech), 100 ng/mL Noggin (Peprotech), penicillin/streptomycin (Gibco), 2.5 µM CHIR99021 (Bioscientific), 10 µM Y-27632 Rock inhibitor (Abcam), 10% R-spondin 1 conditioned media, and 50% WNT3a conditioned media) was added to each well. Organoid forming ability was assessed using the reazurin-based PrestoBlue reagent (Life Technologies), as previously described (12). Cell viability was measured according to the manufacturer's instructions and organoids were imaged using an EVOS FL Auto Cell Imaging System (Invitrogen). Viability was plotted using GraphPad Prism 7, with statistical significance assessed using a Mann Whitney *U* test.

TOPFlash assay

500,000 HEK 293 STF cells were seeded in a 12 well dish for 18 hours. The media was then replaced with 1 mL of pre-warmed media with or without combinations of 1:5 molar ratio of human WNT3a (100 ng/mL, 2.67 nM, StemRD) to toxin (13.35 nM) for 20 hours. Following the incubation, the media was removed and cells were lysed in 110 µL of Passive Lysis Buffer (Promega) for 15 minutes while shaking. The solubilized supernatant was collected and immediately used for the determination of the TOPFlash luciferase activities with the Steady-Glo Luciferase assay (Promega) and CellTiter Glo (Promega).

Treatment of colonic crypts with purified toxins and receptor-blocking proteins, and assessment of organoid formation

Colonic crypts were isolated from C57BL/6J mouse tissues as described previously. The crypt pellets were resuspended in PBS containing 1% FBS and supplemented with 5 nM purified VPI10463TcdB (Abcam) or 100 nM purified RT-027 TcdB. Blocking of toxin variants was conducted with respectively 50 nM or 1000 nM of either recombinant human FZD2 (see above), recombinant human FZD7 Fc chimera (R&D Systems), recombinant human CSPG4 (see above), recombinant

human NECTIN-3 (see above), recombinant human LGR5 Fc chimera (R&D Systems). After four hours at 4°C, the crypt pellets were washed twice with PBS and resuspended in Matrigel (BD), and 12 µL were seeded into each well of a 48-well plate (Nunc) and incubated for 10 minutes at 37°C until solidified. The crypt culture media described above was added to each well. After 3 days, the medium was replaced with fresh culture medium without Y-27632 Rock inhibitor. After four days in culture, cell viability was measured using the PrestoBlue reagent (Life Technologies) and imaged using an EVOS FL Auto Cell Imaging System (Invitrogen). Viability was plotted using GraphPad Prism 7, with statistical significance assessed using a Mann Whitney *U* test.

Treatment of human colonic-organoids with *C. difficile* TcdB

Surgically resected normal colon samples were obtained following written informed consent from four patients at Cabrini hospital, Malvern, Australia. This study was approved by the Cabrini Human Research Ethics Committee (CHREC 04-19-01-15) and the Monash Human Research Ethics committee (MHREC ID 2518 CF15/332-2015000160). Patient recruitment was led by the colorectal surgeons in the Cabrini Monash University Department of Surgery. Tissue was washed and underlying muscle layers were removed with surgical scissors. Tissue was cut into 5 mm pieces and washed eight times in cold chelation buffer (distilled water with 5.6 mM/L Na2HPO4, 8.0 mM/L KH2PO4, 96.2 mM/L NaCl, 1.6 mM/L KCl, 43.4 mM/L sucrose, 54.9 mM/L D-sorbitol). Following incubation for 45 minutes at 4°C in 4 mM EDTA in chelation buffer, intestinal crypts were released from colonic tissue fragments by mechanically pipetting them with a 10 mL pipette in PBS as above. This procedure was repeated a total of three times. Crypts were pelleted by centrifugation at 240*g* for 5 minutes, at 4°C. The crypt pellet was resuspended in PBS, passed through a 100 µm cell strainer and centrifuged. The supernatant was discarded and the pellet containing the crypts was resuspended in matrigel (BD). Matrigel was seeded into each well of a 48 well plate and incubated until solidified. Crypt culture media (advanced DMEM/F12 supplemented with B27 (Gibco), Glutamax (Gibco), N2 (Gibco), 10 mM HEPES (Gibco), 100 µg/mL Primocin (InvivoGen), 100 ng/mL Noggin (Peprotech), 50 ng/ml EGF (Peprotech), 10 nM Gastrin (Sigma Aldrich), 500 nM A83-01 (Torcis), 10 µM SB2002190 (Sigma Aldrich), 2.5 µM CHIR99021 (Bioscientific), 10% R-

spondin 1 conditioned media, and 50% Wnt3a conditioned media) was added to each well. Ten micromoles of Y-27632 dihydrochloride kinase inhibitor (Torcis) was added after initial seeding for two days.

After the establishment of four human colonic-organoid lines, organoids were dissociated using TrypLE Express enzyme (Life technology). After dissociation, cells were pelleted and were resuspended in PBS containing 1% FBS and supplemented with 1 nM purified VPI10463 TcdB (Abcam) or 100 nM purified RT-027 TcdB. Blocking of toxin variants was conducted with 10 nM or 1000 nM of recombinant human FZD7 (R&D Systems), respectively. After four hours at 4°C, the cells were washed twice with PBS and resuspended in Matrigel (BD), and re-seeded into 48 well plates. Organoids were cultured in crypt culture media for eight days before imaging using an EVOS FL Auto Cell Imaging System (Invitrogen). Additionally, cell viability was measured using the PrestoBlue reagent (Life Technologies). The experiments were performed in technical triplicate, per organoid line. Viability was plotted using GraphPad Prism 7, with statistical significance assessed using a One-way ANOVA and Tukey's multiple comparisons test.

Treatment of Vero cells with *C. difficile* TcdB

Vero cells were cultured and prepared as previously described (6). Cells were seeded in 96-well plates at 1×10^4 cells/well, and incubated for 24 hours at 37°C in 5% CO_2. Purified TcdB from strain VPI10463 (Abcam) or purified RT-027 TcdB was diluted in MEM-α containing 1% (v/v) FCS to concentrations of 1 pM, 0.5 pM, and 0.25 pM. Toxin preparations were incubated for 30 minutes on ice with either recombinant human FZD2 (see above), recombinant human FZD7 Fc chimera (R&D Systems), recombinant human CSPG4 (see above), recombinant human NECTIN-3 (see above), recombinant human LGR5 Fc chimera (R&D Systems) or Bovine Serum Albumin (Sigma) each at concentrations of 100 pM, 50 pM, or 25 pM, to give a final ratio of 1:100 toxin:recombinant protein. The toxin or toxin/recombinant protein complexes were added to the Vero cells (100 µL/well) and incubated for four hours prior to removal, rinsing with PBS and replacement with fresh media. Cells treated with media alone were used as negative controls. All conditions were prepared in technical and biological triplicate. Morphological changes were

observed after 18 hours using an Olympus 1X71 inverted microscope at 20x magnification. The cytopathic effect was determined as a percentage of rounded cells in comparison to the negative control wells.

Treatment of HeLa and Caco-2 cells with TcdB

HeLa cells were plated at 7,500 cells per well in a 100 µl volume into 96 well dishes and grown for 18 hours prior to intoxication. Caco-2 cells were plated at 5000 cells per well in a 50 µl volume and grown for 48 hours before intoxication. Cells were maintained in Dulbecco's Modified Eagle's medium (DMEM; Gibco) in 10% fetal bovine serum (FBS; Atlanta Biologicals), and were grown in a humidified incubator at 37 °C with 5% CO_2 atmosphere. HeLa cells were treated with TcdB ($TcdB_{10463}$, $TcdB_{10463}^{GFE}$ and $TcdB_{027}$) for 2.5 hours before measuring viability, while Caco-2 cells were treated for 24 hours before measuring viability by a CellTiterGlo (Promega) viability assay. CellTiterGlo assays were performed according to the manufacturer's protocol and were normalized to untreated conditions. Viability was plotted using GraphPad Prism 7, with statistical significance assessed using a Two-way ANOVA with comparisons made with respect to $TcdB_{10463}$ using Dunnett's multiple comparisons test.

Sequence Analysis and Phylogeny

Fully annotated genomes of *C. difficile* strains deposited on the National Center for Biotechnology Information (NCBI) was used as the source of sequences in this study. As of the time of writing, 78 annotated sequences have been deposited into the NCBI. The *C. difficile* PubMLST database (https://pubmlst.org/cdifficile/) was used to define the *C. difficile* sequence types for these 78 annotated sequences (13, 14). Redundant strains or strains that could not be sequence typed were excluded from sequence analysis. The *tcdB* gene from the unannotated *C. difficile* VPI 10463 strain used in this study was also included in the alignment, amounting to a total of 65 strains for analysis. The loci corresponding to *tcdB* from these 65 strains were translated to determine their TcdB amino acid sequence (15). The TcdB sequences were aligned using the ClustalW algorithm within the R package msa version 1.14.0 (16). The distance and relationships

of these aligned sequences was then determined using the FastME V2 NJ Tree algorithm associated with the GrapeTree Python 2.7 package (17). A dendrogram and alignment was created using the Interactive Tree of Life (18).

Supplementary Appendix

TcdB-producing strains of *C. difficile* induce significant weight loss, diarrhea and colonic epithelial damage

Differences in disease could be seen in the infections with genetically diverse *C. difficile* isolates, with disease severity correlating with the depth of epithelial damage. Infection with M7404, R20291, DLL3109 and VPI1046 resulted in severe disease, inducing ~18% weight loss relative to day zero within 48-hours of infection, limiting animal survival to 48-hours in almost all mice infected with these strains (Fig. S1a i). This heightened disease severity was linked with severe and devastating colonic damage, that penetrated deep into the epithelium, characterized by damage to the base of the colonic crypts, severe inflammation and edema (Fig. S1a) and an eight-point increase in pathology score when compared to tissues isolated from control animals (p=0.0079; Fig. S1a ii). This level of intestinal damage was not seen with CD133, JGS6133, AI35 and 630 infected mice, which had similar pathologies and damage scores to uninfected control mice, all of which were significantly lower than damage score for mice infected with M7404, R20291, DLL3109 and VPI1046 (p>0.05; Fig. S1a ii). M7404, R20291, DLL3109 and VPI1046 were capable of producing significantly higher levels of TcdA and TcdB during infection than CD133, JGS6133, AI35 and 630 ($p<0.05$), which correlated with the level of damage observed for each strain. We suggest that higher toxin production during infection allows for cellular damage to occur at a rate much higher than normal cellular turnover and repair. Thus, damage of the mucosa can then reach the crypt base, exposing the otherwise protected stem cell compartment to intoxication.

To further characterize the progression of epithelial damage and depth of damage during CDI, mice were infected with either M7404 (WT; RT027), or an isogenic mutant strain lacking either TcdA (DLL3045, hereafter $TcdA^{-}B^{+}$), TcdB (DLL3101, hereafter $TcdA^{+}B^{-}$), or TcdA and TcdB (DLL3121, hereafter $TcdA^{-}B^{-}$) (5) and euthanized at either 12, 24 or 48-hours post-infection, to track

the progression of intestinal integrity collapse. Following *C. difficile* challenge with the panel of isogenic M7404 toxin mutants, mice began to lose weight within 12-hours of infection, for each strain tested (Fig. S1b). However, TcdB-producing strains (WT or $TcdA^{-}B^{+}$) induced rapid weight loss at 24 and 48-hours post-infection (Fig. S1b), which coincided with severe diarrhea and extensive colonic epithelial damage (Fig. S1c). By 48-hours of infection, weight loss was significant for all strains tested when compared to the uninfected mice which steadily put on weight (Fig. S1b iii, $p< 0.05$). Notably, WT or $TcdA^{-}B^{+}$ infection induced severe weight loss, up to 15-20% relative to day zero, which was significantly higher than seen for $TcdA^{+}B^{-}$ and $TcdA^{-}B^{-}$ infection (~8% and ~3% respectively; $p<0.05$, Fig. S1c iii).

Consistent with previous results (5), CDT alone ($TcdA^{-}B^{-}$infection) did not play a role in the induction of colonic pathology in this model. Infection with TcdB-producing strains (WT or $TcdA^{-}B^{+}$) induced severe and extensive colonic epithelial damage that was most severe 48-hours post-infection (Fig. S1c, d). Specifically, colon pathology scores were significantly higher for infection with TcdB-producing strains than in mice infected with TcdB-negative ($TcdA^{+}B^{-}$ and $TcdA^{-}B^{-}$) strains or uninfected mice, characterized by extensive mucosal damage, inflammation and edema in WT or $TcdA^{-}B^{+}$-infected mice (Fig. S1c, d; $p<0.05$). These disease features were absent in mice infected with TcdB-negative strains, except for weight loss, which occurred at lower levels than infection with TcdB-producing strains (Fig. S1b).

TcdB induces colonic epithelial apoptosis during CDI

Since CDI induces extensive damage and inflammation throughout the colonic epithelium (Fig. S1c), we examined if the stem cell compartment, located at the base of the crypts, was being targeted during infection. Colonic tissue was examined for apoptosis by staining for activated caspase-3 and total numbers of apoptotic cells throughout the epithelium and at the base of the crypts (Fig. S2). These results suggest that TcdB, but not TcdA, is responsible for causing colonic epithelial cell apoptosis, as infection with TcdB-producing strains increases apoptosis at the crypt base, where the stem cell population resides, which may have a profound effect on stem cell function and the capacity for tissue regeneration following CDI.

Infection with WT and TcdA$^-$B$^+$ strains resulted in a significant increase in total cellular apoptosis throughout the colonic crypts when compared to uninfected mice at 24-hours (p=0.0159) and 48-hours (p=0.0260 and p=0.001, respectively) and to TcdA$^-$B$^-$ infection at 24-hours (p=0.0159) and 48-hours (p=0.0346 and p=0.001, respectively; Fig. S2). In contrast, the TcdA$^+$B$^-$ strain did not cause apoptosis above levels observed for uninfected mice or in TcdA$^-$B$^-$ infected mice, and induced significantly less total apoptosis when compared to WT and TcdA$^-$B$^+$ infection at 48-hours (p=0.043 and p=0.001, respectively; Fig. S2). Importantly, at the later time point of infection with WT and TcdA$^-$B$^+$ strains, the levels of apoptosis at the crypt base, where the stem cell population resides, had significantly increased in comparison to uninfected mice (p=0.011 for TcdA$^-$B$^+$ infection only) and to TcdA$^-$B$^-$ (p=0.0368 and p=0.0025, respectively) and TcdA$^+$B$^-$ infection (p=0.013 and p=0.0025, respectively; Fig. S2).

TcdB alters stem cell signaling and gene transcription during CDI

As TcdB appears to damage cells within the base of the colonic crypt (Fig. S2), and stem cell function appears to be altered by TcdB (Fig. 2 a) we next examined the effect that this may have on stem cell signaling. Quantitative digital droplet-PCR (ddPCR) was performed using seven genes that are representative markers of stem cells (*Bmi1*, *Ascl2*, *Ephb2* and *Lgr5*), WNT-signaling (*Axin2* and *Fzd7*) and cellular proliferation (*c-myc*), and the results normalized to uninfected mice (Figure 2b). Gene expression was altered across all strains of infection, with significant alterations in gene expression observed following TcdB mediated damage.

The role of TcdB in disrupting the stem cell compartment can also be clearly seen upon comparison of mice infected with TcdB-producing strains to those infected with the TcdA$^+$B$^-$ strain, at 24-hours. Here, WT-infected mice expressed significantly less *Axin2* (p=0.0159), *Lgr5* (p=0.0286) and *Fzd7* (p=0.286) when compared to TcdA$^+$B$^-$ infected mice (Fig. 2b i). When compared to TcdA$^-$B$^-$ infected mice at 24-hours, WT-infected mice also expressed significantly less *Ascl2, Axin2, Fzd7* and *Lgr5* ($p<0.05$). TcdA$^-$B$^+$-infected mice showed similar low levels of stem cell gene expression to WT-infected mice, however significance was only seen when comparing *Lgr5* expression to TcdA$^-$B$^-$-infected mice (p=0.0357) and *Fzd7* to TcdA$^+$B$^-$-infected mice (p=0.0357). By

48-hours of infection, the effects of TcdB-producing strains on stem cell and WNT-signaling markers were more pronounced, with significantly reduced expression of *Ascl2, Axin2, Bmi1, Fzd7* and *Lgr5* ($p<0.05$) detected in WT-infected mice as well as a significant reduction in *Axin2* ($p=0.0317$), *Bmi1* ($p=0.0317$) and *Lgr5* ($p=0.0357$) in $TcdA^-B^+$-infected mice compared to $TcdA^-B^-$-infected mice (Fig. 2b ii). TcdA does not appear to alter the stem cell compartment or WNT-signaling 48-hours post-infection since similar levels of gene expression were detected in mice infected with $TcdA^+B^-$ and $TcdA^-B^-$ strains, and WT-infected mice expressed significantly less *Ascl2, Axin2*, *Bmi1, Fzd7* and *Lgr5* ($p<0.05$) in comparison to those infected with the $TcdA^+B^-$ strain (Fig. 2b ii). Furthermore, comparison of $TcdA^-B^+$ infection to $TcdA^+B^-$ infection at 48-hours showed that there was a significant reduction in expression of the stem cell genes/markers *Axin2* and *Lgr5* ($p=0.0317$ and $p=0.0159$, respectively; Fig. 2b ii), and expression of *EphB2* and *Fzd7* less than half that detected for $TcdA^+B^-$ infection, providing further evidence that TcdB is disrupting the stem cell compartment.

TcdB receptors are expressed at high levels in the colonic LGR5 stem cells and their daughter cells

To assess the expression of known TcdB receptors in the cells of the colonic epithelium, and in particular the colonic stem cells and stem cell niche, we separated and sorted cells from colons of adult LGR5-eGFP-IRES-CreERT2 mice (11). Cells were sorted into LGR5 negative, low, medium and high or epithelial cell populations and qPCR was performed to examine the expression levels of TcdB receptors *Fzd7, Lrp1* and *Nectin3*. As expected, *Lgr5* expression was highest in the LGR5-GFP high cells ($p<0.0001$), and decreased in expression relative to LGR5-GFP levels ($p<0.05$; Fig. S3). Interestingly, both *Fzd7* and *Nectin3* were expressed at levels equivalent to *Lgr5* in the LGR5-GFP high colonic stem cells ($p<0.001$; Fig. S3). *Fzd7* expression was also high in the LGR5-GFP medium cell population, which includes progenitor cells of the colon ($p<0.05$; Extended Data Fig.3). Unlike *Fzd7* and *Nectin3* the TcdB co-receptor *Lrp1* was expressed at a consistent level throughout the LGR5 low, medium and high or epithelial cell populations, and highly expressed in the LGR5-GFP negative population ($p<0.0001$; Fig. S3). As LRP1 acts as an

468 "internalizing receptor" (19), consistent expression throughout the colonic epithelium may assist
469 TcdB internalization throughout various cells within the epithelial layer.

470 **RT027 TcdB induces epithelial damage and stem cell death without binding to FZD receptors**

471 Although $TcdB_{027}$ was shown not to bind FZD proteins *in vitro* (Fig 4a), $TcdB_{027}$ was still
472 able to induce stem cell death and dysfunction *in vivo* (Fig. 2). To confirm that all TcdB types used
473 in our binding assays were indeed functional, we utilized a rectal instillation mouse toxicity model,
474 and examined $TcdB_{10463}$, $TcdB_{027}$ and $TcdB_{10463}^{GFE}$ for their ability to induce severe colonic damage.
475 All three toxins were able to induce severe colonic damage, deep into the colonic mucosa, with
476 damage down to the base of the crypts where the stem cells reside (Fig. S4c). Specifically, tissues
477 from mice treated with $TcdB_{10463}$, $TcdB_{027}$ and $TcdB_{10463}^{GFE}$ displayed large regions of hyperplasia,
478 severe inflammation into both the mucosa and submucosa and a large amount of edema, when
479 compared to the control tissues, which was reflected in the significantly higher histopathological
480 scores of intoxicated mice ($p<0.05$; Fig. S4c). As both $TcdB_{10463}$ and$TcdB_{027}$ induce similar levels
481 of damage, it appears that FZD binding may not be essential to induce stem cell death and
482 dysfunction. To test this theory, we isolated crypts from uninfected mice, and intoxicated with
483 purified $TcdB_{10463}$ and $TcdB_{027}$ toxins for four hours, before washing, and using these intoxicated
484 cells for organoid culture. If unintoxicated, stem cells will remain viable and produce mature
485 organoids in this culture system. Indeed, both toxins were capable of inhibiting organoid
486 establishment, highlighting that TcdB can induce stem cell death and dysfunction irrespective of
487 FZD binding, with multiple receptor binding pathways likely to induce stem cell death (Fig. 3b). This
488 was confirmed by the partial blockage of $TcdB_{10463}$ but not $TcdB_{027}$ mediated stem cell death by
489 FZD2 and FZD7, suggesting that TcdB has adapted several mechanisms to target these cells.

490 **$TcdB_{10463}$ and $TcdB_{027}$ dose response in murine organoids**

491 To examine the differential receptor binding of $TcdB_{10463}$ and $TcdB_{027}$ in the context of our
492 *in vivo* infection data, receptor blocking experiments were performed. Previous work with each toxin
493 had determined a broad range of concentrations that could induce murine colonic epithelial cell
494 death. To further define the concentration at which $TcdB_{10463}$ and $TcdB_{027}$ induces murine stem cell

death, we performed a dose response from 0.5 nM to 10 nM for $TcdB_{10463}$ and 1 nM to 100 nM for $TcdB_{027}$ (Fig S5a). Crypts from uninfected mice were isolated and intoxicated with purified $TcdB_{10463}$ and $TcdB_{027}$ toxins for 4 hours, before washing and using in organoid seeding. After 7 days, organoid viability was measured, to establish at what concentration each toxin could induce near complete stem cell death. These data indicated that 5 nM of $TcdB_{10463}$ and 100 nM of $TcdB_{027}$ were sufficient to induce a similar level of stem cell death, without complete ablation of organoid seeding, with organoid viability counts around 10% of that detected for untreated control organoids (Fig S5a).

C. difficile **mediated stem cell dysfunction induces long effects on intestinal repair**

Taken together, our data show that $TcdB_{027}$ induces severe and devastating epithelial damage deep into the mucosa, which damages the colonic stem cell compartment, altering their regenerative capacity at the peak of infection. However, the impact of this dysfunction on long term repair has not been explored. To assess this gap in enteric infection literature, we assessed mice that were infected with *C. difficile,* that reached a peak of infection, and then allowed them to recover, to two weeks post the peak of infection. Infected recovery mice began to steadily put on weight over the two weeks of recovery, reaching weights close to those measured pre-infection. However, this was significantly less than uninfected mice taken at the same time point, which had increased in weight by ~6%. As these mice were not treated with antibiotics to clear their infection we did not expect a complete cessation in *C. difficile* shedding. Interestingly, levels of *C. difficile* shedding had significantly dropped from ~$5x10^6$ CFU/100mg feces at the peak of infection, to less than $5x10^3$ CFU/100mg feces two weeks post peak of infection. This correlated with a significant decrease in TcdB detection, with less than 1ng TcdB/100mg feces detectable at two weeks post peak of infection, compared to >50ng TcdB/100mg feces at the peak of infection. Despite the recovery and significant clearance of *C. difficile* in our infected mice, significant colonic tissue damage and stem cell dysfunction were still apparent when compared to uninfected mice (Fig. 4), highlighting that CDI has long term effects on stem cell function, which delay the recovery process.

Table S1. Strains and Characteristics.

Strain	Characteristics	Reference
M7404	*tcdA*$^+$/*tcdB*$^+$/*cdtAB*$^+$, Clade 2, Ribotype 027, human clinical isolate, Canada, 2005.	(20)
DLL3045 (TcdA$^-$B$^+$)	M7404 derivative (M7404 *tcdA* TargeTron) *tcdA*$^-$/*tcdB*$^+$/*cdtAB*$^+$	
DLL3101 (TcdA$^+$B$^-$)	M7404 derivative (M7404Ω*tcdB* TargeTron) *tcdA*$^+$/*tcdB*$^-$/*cdtAB*$^+$	(5)
DLL3121 (TcdA$^-$B$^-$)	M7404 derivative (M7404Ω*tcdA* TargeTron, Ω *tcdB* TargeTron), *tcdA*$^-$/*tcdB*$^-$/*cdtAB*$^+$.	(5)
R20291	*tcdA*$^+$/*tcdB*$^+$/*cdtAB*$^+$, Clade 2, Ribotype 027, human clinical isolate, United Kingdom, 2006.	(21)
DLL3109	*tcdA*$^+$/*tcdB*$^+$/*cdtAB*$^+$, Clade 2, Ribotype 027, human clinical isolate, Australia, 2010.	(22-24)
VPI10463	*tcdA*$^+$/*tcdB*$^+$/*cdtAB*$^-$, Clade 1, Ribotype 003, Human isolate, reference strain, America, before 1982.	(25, 26)
630	*tcdA*$^+$/*tcdB*$^+$/*cdtAB*$^-$, Clade 1, Ribotype 012, human clinical isolate, Switzerland, 1982.	(27, 28)
JGS6133	*tcdA*$^+$/*tcdB*$^+$/*cdtAB*$^+$, Clade 5, Ribotype 078, porcine isolate, America, before 2013.	(29)
AI35	*tcdA*$^-$/*tcdB*$^+$(variant)/*cdtAB*$^+$, Clade 5, Ribotype 237, porcine isolate, Australia, 2013.	(29)
CD133	*tcdA*$^-$/*tcdB*$^-$/*cdtAB*$^-$, Clade 1, AUS-ribotype 091*, human clinical isolate, Australia, 2008.	This Study

*AUS-ribotyping

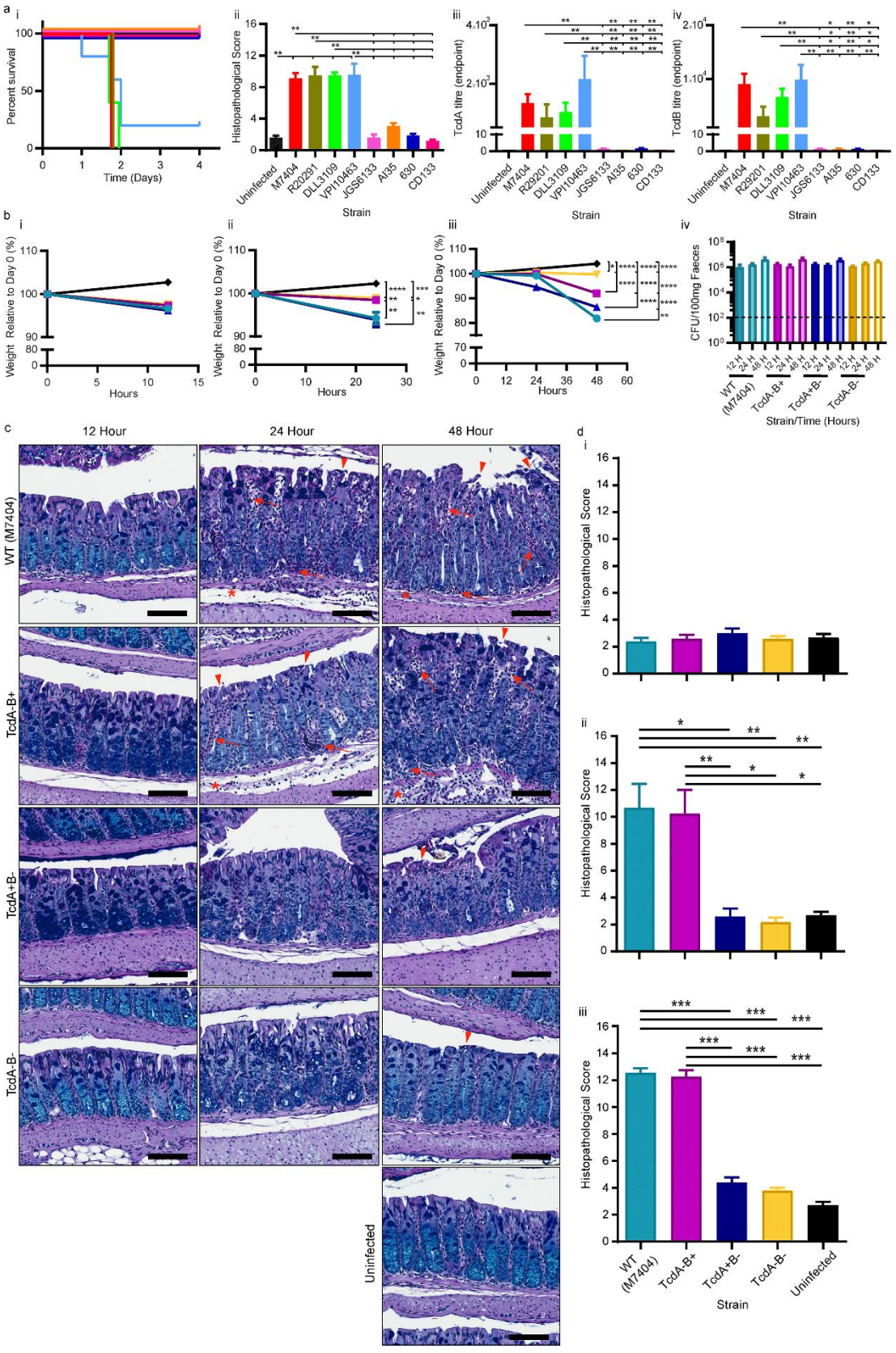
a
i
Percent survival
Time (Days)
ii
Histopathological Score
iii
TcdA titre (endpoint)
iv
TcdB titre (endpoint)
Uninfected
M7404
R20291
DLL3109
VPI10463
JGS6133
AI35
630
CD133
Strain
b
i
ii
iii
iv
Weight Relative to Day 0 (%)
Hours
CFU/100mg Faeces
WT (M7404)
TcdA-B+
TcdA+B-
TcdA-B-
Strain/Time (Hours)
c
12 Hour
24 Hour
48 Hour
WT (M7404)
TcdA-B+
TcdA+B-
TcdA-B-
Uninfected
d
i
ii
iii
Histopathological Score
Strain

524

Fig. S1. *C. difficile* induces severe and deep epithelial damage and weight loss, predominantly though TcdB. a) Mice were infected with a panel of genetically distinct *C. difficile* isolates and monitored for disease severity and weight loss. Mice that lost >10% body weight within 24-hours of >15% thereafter were euthanized. **i)** Kaplan-Meier survival curve, **ii)** Representative PAS/Alcian blue stained colonic tissue collected and scored at time of euthanasia, **iii)** TcdA titer of fecal samples tested on HT29 cells, and **iv)** TcdB titer of fecal samples tested on Vero cells. **b)** C57BL/6J mice were challenged with M7404 (WT) (teal), $TcdA^{-}B^{+}$ (fuchsia), $TcdA^{+}B^{-}$ (blue), and $TcdA^{-}B^{-}$ (yellow) isogenic *C. difficile* spores or left uninfected (black), euthanizing separate groups at 12, 24 or 48-hours post-infection. Weight loss relative to day zero for individual groups following infection or uninfected mice euthanized at **i)** 12-hours, **ii)** 24-hours and **iii)** 48-hours post-infection. **iv)** Fecal spore shedding of *C. difficile* at time of euthanasia. **c)** Representative PAS/Alcian blue stained colonic tissue collected at 12, 24 and 48-hours post-infection with WT, $TcdA^{-}B^{+}$, $TcdA^{+}B^{-}$, and $TcdA^{-}B^{-}$ *C. difficile* or from uninfected mice (48-hours). Arrow=Inflammation; Arrowhead=crypt damage/goblet cell loss; Asterisk=Edema. Scale bar = 100 µm. **d)** Histopathological scores for **i)** 12-hours, **ii)** 24-hours and **iii)** 48-hours post-infection were plotted. n≥5. * $p \leq 0.05$, ** $p \leq 0.01$, *** $p \leq 0.001$, **** $p \leq 0.0001$. See also Fig. 1.

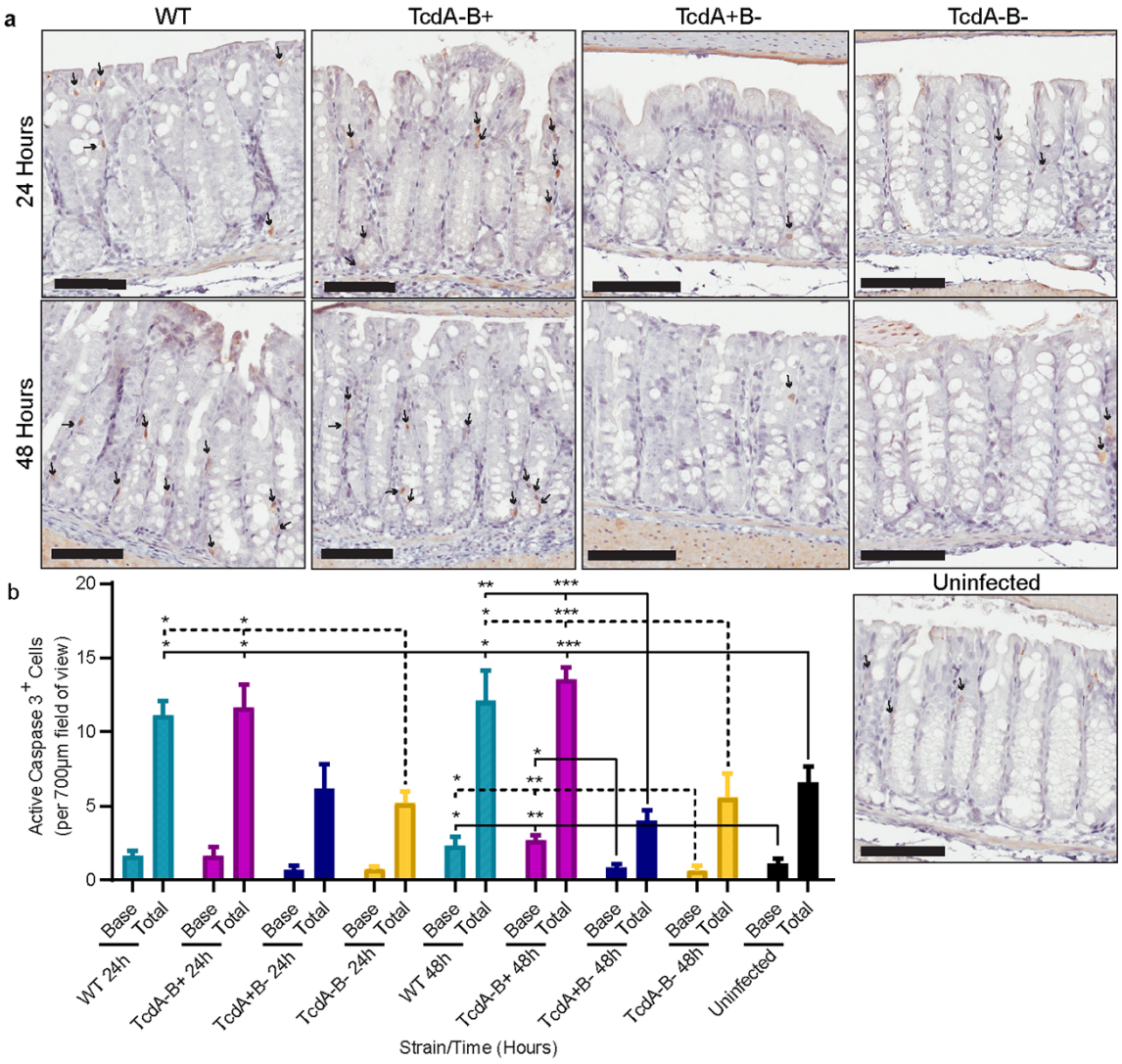

Fig. S2. *C. difficile* infection induces epithelial cell apoptosis, which is associated with infection with TcdB-producing strains. Colonic tissues were collected at 24 and 48-hours post-infection with WT, TcdA$^-$B$^+$, TcdA$^+$B$^-$, and TcdA$^-$B$^-$ *C. difficile* strains and from uninfected mice (48-hours). **a)** Representative images of tissues stained for activated caspase-3 (brown cells and arrow). **b)** Activated caspase-3 cell counts per 700 µm field of view are shown. n≥5, Scale Bar = 100 µm. Data are represented as mean + S.E.M. * p≤ 0.05, ** p≤ 0.01, *** p≤ 0.001. See also, Fig. 2.

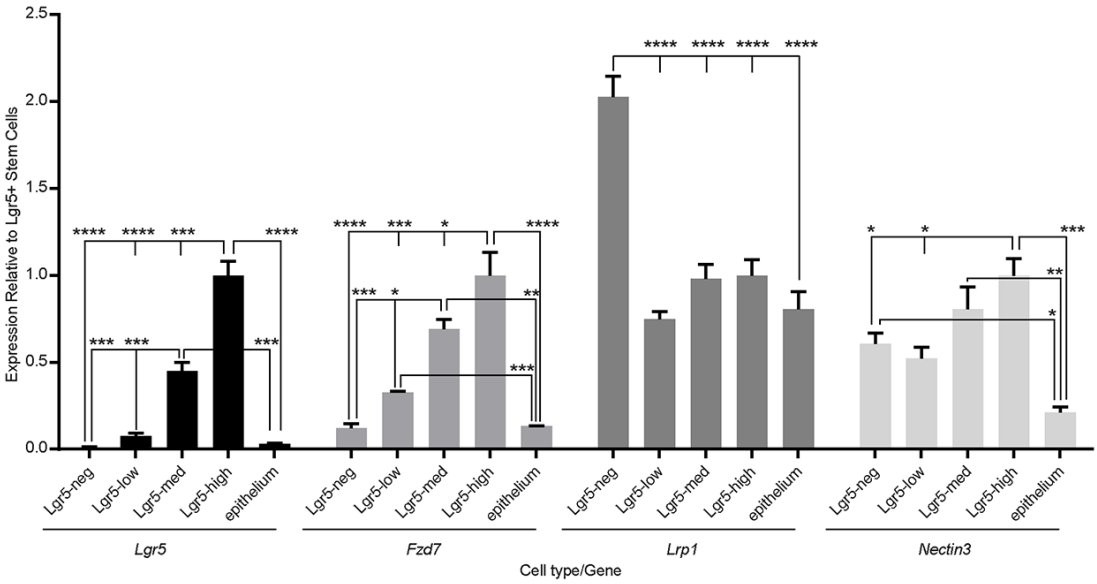

551

552 **Fig. S3. Colonic stem cells and their daughter cells express TcdB receptors**. Colonic cells
553 from adult LGR5-eGFP-IRES-CreERT2 mice were isolated, stained and sorted prior to RNA
554 isolation and cDNA synthesis. qPCR was then used to quantify the expression levels of *Lgr5, Fzd7,*
555 *Lrp1* and *Nectin3* in differentiated cells (LGR5-neg), progenitor cells (LGR5-low and LGR5 medium
556 (med)), colonic stem cells (LGR5-high) and total epithelial cells. n=3. Data are represented as mean
557 + S.E.M * $p \leq 0.05$, ** $p \leq 0.01$, *** $p \leq 0.001$, **** $p \leq 0.0001$. See also, Fig. 3.

558

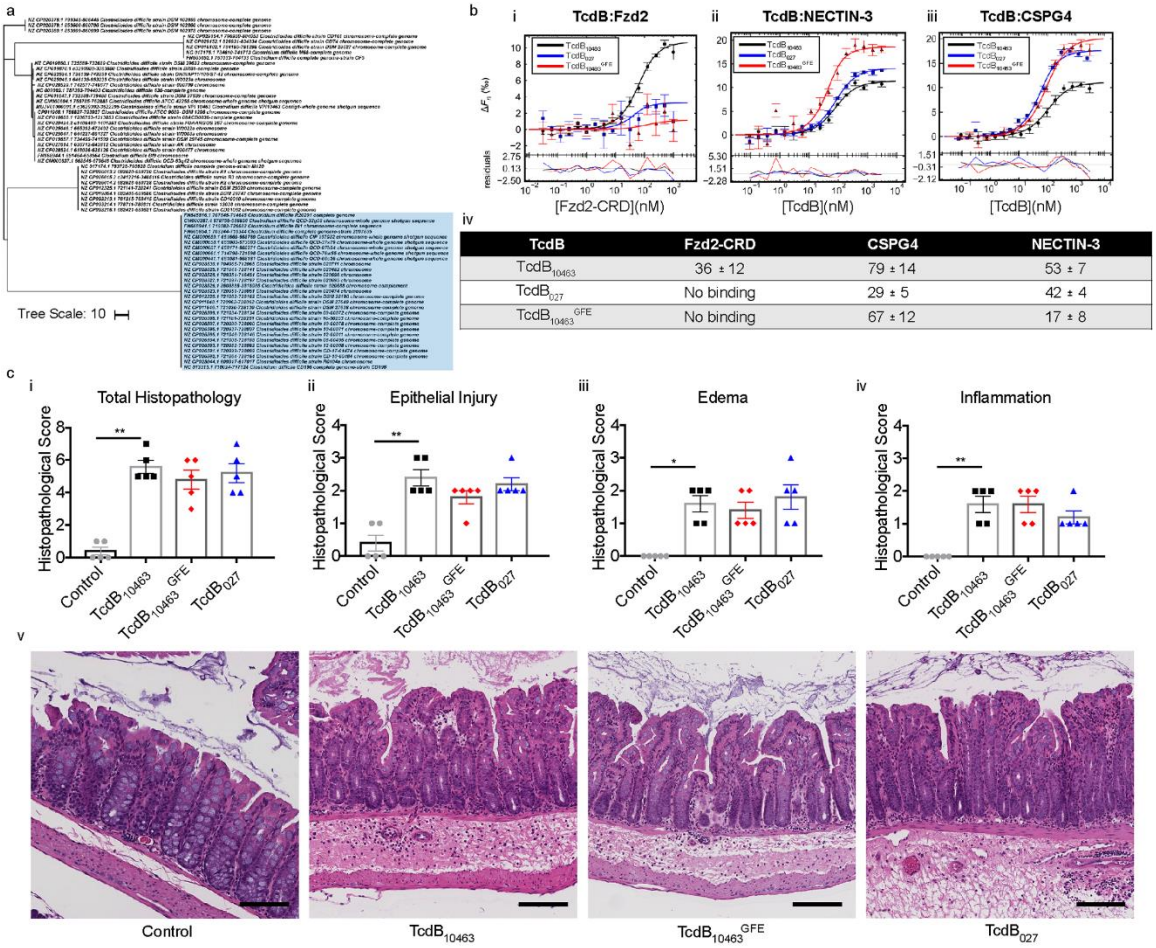

559

560 **Fig. S4. TcdB$_{027}$ does not bind FZD proteins, but still induces severe colonic damage. a)** A
561 phylogenetic tree was generated from an alignment of TcdB amino acid sequences from annotated
562 *C. difficile* genomes deposited in NCBI. The blue shade highlights RT027 strains of *C. difficile* and
563 reveals that these strains have identical TcdB sequences. **b)** Microscale thermophoresis (MST)
564 responses with TcdBs titrated against a 16-step serial dilution of **i)** FZD2-CRD, **ii)** NECTIN-3 and
565 **iii)** CSPG4 titrated against serial dilutions of TcdBs. Curves were fit to a one-site binding model to
566 determine K_D values (nM). The confidence intervals were calculated from three independent
567 experiments in PALMIST using the variance-covariance method. **iv)** K_D values between TcdBs and
568 their receptors determined by MST. **c)** Individual scoring of mice colon exposed for 4 hours with
569 PBS or 50 µg TcdB as described by **i)** total histopathology, **ii)** epithelial injury, **iii)** edema, and **iv)**
570 inflammation. **v)** Representative H&E images of tissue from mice injected with either PBS or 50 µg

of TcdB. Scale bar = 100 µM. n=5. Data are represented as mean + S.E.M. * p≤ 0.05, ** p≤ 0.01, One-way Kruskal-Wallis with Dunn's post-hoc test for multiple comparisons. See also Fig. 3.

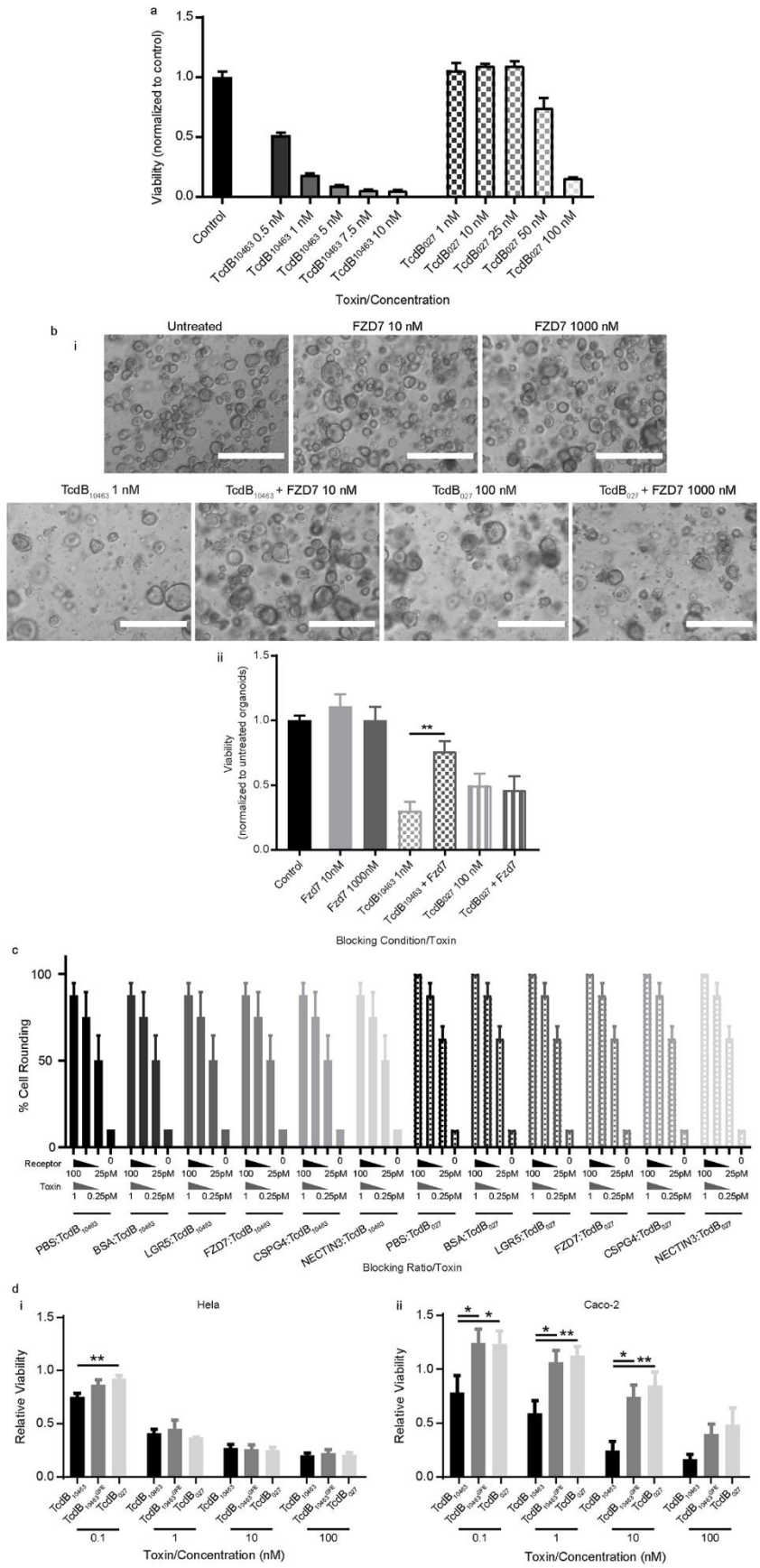
a
Viability (normalized to control)
Control
TcdB10463 0.5 nM
TcdB10463 1 nM
TcdB10463 5 nM
TcdB10463 7.5 nM
TcdB10463 10 nM
TcdB027 1 nM
TcdB027 10 nM
TcdB027 25 nM
TcdB027 50 nM
TcdB027 100 nM
Toxin/Concentration
b
i
Untreated
FZD7 10 nM
FZD7 1000 nM
TcdB10463 1 nM
TcdB10463 + FZD7 10 nM
TcdB027 100 nM
TcdB027 + FZD7 1000 nM
ii
Viability (normalized to untreated organoids)
Control
Fzd7 10nM
Fzd7 1000nM
TcdB10463 1nM
TcdB10463 + Fzd7
TcdB027 100 nM
TcdB027 + Fzd7
Blocking Condition/Toxin
c
% Cell Rounding
Receptor
Toxin
PBS:TcdB10463
BSA:TcdB10463
LGR5:TcdB10463
FZD7:TcdB10463
CSPG4:TcdB10463
NECTIN3:TcdB10463
PBS:TcdB027
BSA:TcdB027
LGR5:TcdB027
FZD7:TcdB027
CSPG4:TcdB027
NECTIN3:TcdB027
Blocking Ratio/Toxin
d
i
Hela
Relative Viability
Toxin/Concentration (nM)
ii
Caco-2
Relative Viability
Toxin/Concentration (nM)

Fig. S5. $TcdB_{10463}$ and $TcdB_{027}$ can bind to cells in FZD dependent and independent mechanisms. a) Equal numbers of colonic crypts were isolated from uninfected mice and then exposed to a range of $TcdB_{10463}$ and $TcdB_{027}$ doses (0.5 – 10 nM and 1 – 100 nM, respectively) to identify a suitable dose for intoxication blocking experiments. **b)** Equal numbers of dissociated human colonic organoid cells were exposed to toxin, with or without recombinant FZD7 prior to organoid seeding. **i)** Representative images of organoids at day eight cultured from cells incubated for four hours with 1 nM of $TcdB_{10463}$ or 100 nM $TcdB_{027}$. Blocking was conducted with 10nM or 1000 nM, respectively, of recombinant FZD7. Untreated controls and organoids treated with FZD7 alone are shown; n=4, scale bar = 400 µM. **ii**) cell viability, as assessed *via* a PrestoBlue assay, was measured at day eight post seeding. Data are represented as mean + S.E.M. ** p≤ 0.01, One-way ANOVA, Tukey's multiple comparison test. **c)** Vero cells seeded at 10^4 cells per well were cultured following a four-hour exposure to $TcdB_{10463}$ and $TcdB_{027}$ that was treated with either PBS, BSA, or recombinant receptor using a range of TcdB concentrations (1 pM, 0.5 pM and 0.25 pM) in a ratio of 1:100 of toxin to added protein or left untreated (media alone). **d)** Hela and Caco-2 cells seeded at 7.5 x 10^3 and 5 x 10^3 cells per well, respectively, were cultured following exposure to $TcdB_{10463}$ (black), $TcdB_{10463}^{GFE}$ (dark grey), and $TcdB_{027}$ (light grey) at a range of concentrations (0.1 nM, 1 nM, 10 nM and 100 nM). Cell viability was measured using an ATP viability indicator (CellTiterGlo) at **i)** 2.5 hours of exposure on Hela cells or **ii)** 24 hours on Caco-2 cells. n = 3; Data are represented as mean + S.E.M. * p≤ 0.05, ** p≤ 0.01, Two-way Kruskal-Wallis with Dunn's post-hoc test for multiple comparisons. See also Fig. 3.

References

1. R. Chandrasekaran, A. K. Kenworthy, D. B. Lacy, *Clostridium difficile* Toxin A Undergoes Clathrin-Independent, PACSIN2-Dependent Endocytosis. *PLoS Pathog* **12**, e1006070 (2016).
2. T. Loo, M. L. Patchett, G. E. Norris, J. S. Lott, Using secretion to solve a solubility problem: high-yield expression in *Escherichia coli* and purification of the bacterial glycoamidase PNGase F. *Protein Expr. Purif.* **24**, 90-98 (2002).
3. T. H. Scheuermann, S. B. Padrick, K. H. Gardner, C. A. Brautigam, On the acquisition and analysis of microscale thermophoresis data. *Anal. Biochem.* **496**, 79-93 (2016).
4. S. A. Lyon, M. L. Hutton, J. I. Rood, J. K. Cheung, D. Lyras, CdtR regulates TcdA and TcdB production in *Clostridium difficile*. *PLoS Pathog* **12**, e1005758 (2016).
5. G. P. Carter *et al.*, Defining the roles of TcdA and TcdB in localized gastrointestinal disease, systemic organ damage, and the host response during *Clostridium difficile* infections. *mBio* **6** (2015).
6. D. Lyras *et al.*, Toxin B is essential for virulence of *Clostridium difficile*. *Nature* **458**, 1176-1179 (2009).
7. C. M. Theriot *et al.*, Cefoperazone-treated mice as an experimental platform to assess differential virulence of *Clostridium difficile* strains. *Gut Microbes* **2**, 326-334 (2011).
8. T. Jarde *et al.*, *In vivo* and *in vitro* models for the therapeutic targeting of Wnt signaling using a Tet-ODeltaN89beta-catenin system. *Oncogene* **32**, 883-893 (2013).
9. C. M. Nefzger *et al.*, A Versatile Strategy for Isolating a Highly Enriched Population of Intestinal Stem Cells. *Stem Cell Reports* **6**, 321-329 (2016).
10. T. Jarde, G. Kerr, R. Akhtar, H. E. Abud, Modelling Intestinal Carcinogenesis Using *In Vitro* Organoid Cultures. *Methods Mol. Biol.* **1725**, 41-52 (2018).
11. N. Barker *et al.*, Identification of stem cells in small intestine and colon by marker gene *Lgr5*. *Nature* **449**, 1003-1007 (2007).

12. K. Horvay *et al.*, Snai1 regulates cell lineage allocation and stem cell maintenance in the mouse intestinal epithelium. *EMBO J.* **34**, 1319-1335 (2015).
13. D. Griffiths *et al.*, Multilocus sequence typing of *Clostridium difficile*. *J. Clin. Microbiol.* **48**, 770-778 (2010).
14. K. A. Jolley, M. C. Maiden, BIGSdb: Scalable analysis of bacterial genome variation at the population level. *BMC Bioinformatics* **11**, 595 (2010).
15. P. Stothard, The sequence manipulation suite: JavaScript programs for analyzing and formatting protein and DNA sequences. *Biotechniques* **28**, 1102, 1104 (2000).
16. U. Bodenhofer, E. Bonatesta, C. Horejs-Kainrath, S. Hochreiter, msa: an R package for multiple sequence alignment. *Bioinformatics* **31**, 3997-3999 (2015).
17. Z. Zhou *et al.*, GrapeTree: visualization of core genomic relationships among 100,000 bacterial pathogens. *Genome Res.* **28**, 1395-1404 (2018).
18. I. Letunic, P. Bork, Interactive Tree Of Life (iTOL) v4: recent updates and new developments. *Nucleic Acids Res* 10.1093/nar/gkz239 (2019).
19. D. Schottelndreier *et al.*, Expression and (Lacking) Internalization of the Cell Surface Receptors of *Clostridioides difficile* Toxin B. *Front Microbiol* **9**, 1483 (2018).
20. G. P. Carter *et al.*, Binary toxin production in *Clostridium difficile* is regulated by CdtR, a LytTR family response regulator. *J. Bacteriol.* **189**, 7290-7301 (2007).
21. R. A. Stabler *et al.*, Comparative genome and phenotypic analysis of *Clostridium difficile* 027 strains provides insight into the evolution of a hypervirulent bacterium. *Genome Biol* **10**, R102 (2009).
22. G. P. Carter *et al.*, The anti-sigma factor TcdC modulates hypervirulence in an epidemic BI/NAP1/027 clinical isolate of *Clostridium difficile*. *PLoS Pathog* **7**, e1002317 (2011).
23. M. Richards *et al.*, Severe infection with *Clostridium difficile* PCR ribotype 027 acquired in Melbourne, Australia. *Med. J. Aust.* **194**, 369-371 (2011).
24. S. K. Lim *et al.*, Emergence of a ribotype 244 strain of *Clostridium difficile* associated with severe disease and related to the epidemic ribotype 027 strain. *Clin. Infect. Dis.* **58**, 1723-1730 (2014).

25. J. F. Torres, I. Lonnroth, Purification and characterisation of two forms of toxin B produced by *Clostridium difficile*. *FEBS Lett.* **233**, 417-420 (1988).
26. N. M. Sullivan, S. Pellett, T. D. Wilkins, Purification and characterization of toxins A and B of *Clostridium difficile*. *Infect Immun* **35**, 1032-1040 (1982).
27. J. Wust, N. M. Sullivan, U. Hardegger, T. D. Wilkins, Investigation of an outbreak of antibiotic-associated colitis by various typing methods. *J. Clin. Microbiol.* **16**, 1096-1101 (1982).
28. J. Wust, U. Hardegger, Transferable resistance to clindamycin, erythromycin, and tetracycline in *Clostridium difficile*. *Antimicrob. Agents Chemother.* **23**, 784-786 (1983).
29. M. M. Squire *et al.*, Novel molecular type of *Clostridium difficile* in neonatal pigs, Western Australia. *Emerg. Infect. Dis.* **19**, 790-792 (2013).